

TAFE-Net: Task-Aware Feature Embeddings for Efficient Learning and Inference

Xin Wang Fisher Yu Ruth Wang Trevor Darrell Joseph E. Gonzalez
EECS Department, UC Berkeley

Abstract

Learning good feature embeddings for images often requires substantial training data. As a consequence, in settings where training data is limited (e.g., few-shot and zero-shot learning), we are typically forced to use a general feature embedding across prediction tasks. Ideally, we would like to construct feature embeddings that are tuned for the given task and even input image. In this work, we propose Task-Aware Feature Embedding Networks (TAFE-Nets) to learn how to adapt the image representation to a new task in a meta learning fashion. Our network is composed of a meta learner and a prediction network, where the meta learner generates parameters for the feature layers in the prediction network based on a task input so that the feature embedding can be accurately adjusted for that task. We show that our TAFE-Net is highly effective in generalizing to new tasks or concepts and offers efficient prediction with low computational cost. We demonstrate the general applicability of TAFE-Net in several tasks including zero-shot/few-shot learning and dynamic efficient prediction. Our networks exceed or match the state-of-the-art on most tasks. In particular, our approach improves the prediction accuracy of unseen attribute-object pairs by 4 to 15 points on the challenging visual attributes composition task.

1. Introduction

Feature embeddings are central to computer vision. By mapping images into semantically rich vector spaces, feature embeddings extract key information that can be used for a wide range of prediction tasks. However, learning good feature embeddings typically requires substantial amounts of training data and computation. As a consequence, a common practice [7, 12, 49] is to re-use existing feature embeddings from convolutional networks (e.g., ResNet50 [18]) trained on large-scale labeled training datasets (e.g., ImageNet [35]); to achieve maximum accuracy, these general feature embedding are often fine-tuned [12, 7, 49] or transformed [20] using additional task specific training data.

In many settings, the training data are insufficient to learn

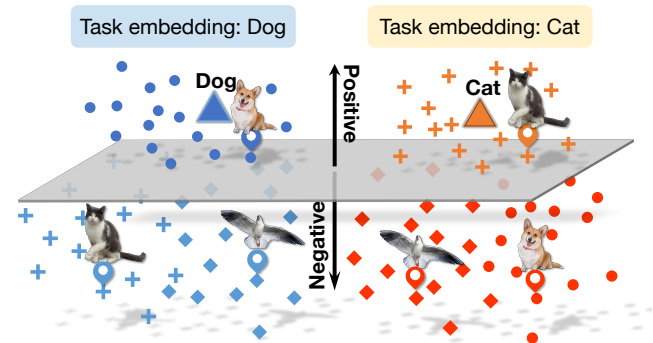


Figure 1: A cartoon illustration of Task-aware Feature Embedding. In this case there are two binary prediction tasks (hasCat and hasDog). Task-aware feature embeddings mean that the same image can have different embeddings for each task. As a consequence, we can adopt a single task independent classification boundary for all tasks.

or even adapt general feature embeddings to a given task. For example, in few-shot and zero-shot prediction tasks, the scarcity of training data forces the use of generic feature embeddings. As a consequence, in these situations much of the research instead focuses on the design of joint task and data embeddings [4, 11, 51] that can be generalized to unseen tasks or tasks with fewer examples. Some have proposed treating the task embedding as linear separators and learning to generate them for new tasks [41, 29]. Others have proposed hallucinating additional data points [47, 17, 44]. However, in all cases, a common image embedding is shared across tasks. As a consequence, the common image embedding may be out of the domain or sub-optimal for any individual prediction task. This problem is exacerbated in settings where the number and diversity of training tasks is relatively small.

In this work we explore a meta-learning approach to constructing task-aware feature embeddings (TAFE). We introduce task-aware feature embedding networks (TAFE-Nets¹) composed of a task-aware meta learner that generates the

¹Pronounced taffy-nets

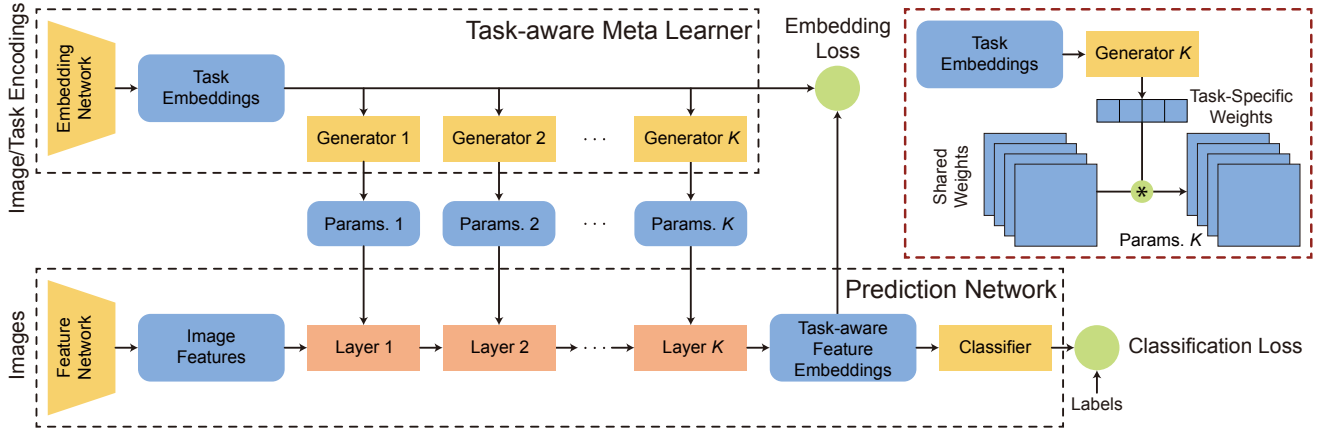


Figure 2: TAFE-Net architecture design. TAFE-Net has a task-aware meta learner that generates the parameters of the feature layers within a prediction network for classification. The generated weights are factorized into task-specific weights in low dimension and shared weights across all tasks.

parameters for feature embedding layers within a standard prediction network. As a consequence, we are able to learn a simple task-independent linear boundary that can separate the positive and negative examples through the use of the task aware feature embeddings. To address the challenge of meta-learning with limited numbers of training tasks, we couple the task embedding to the task aware feature embeddings with the addition of a novel embedding loss. The resulting coupling improves generalization across tasks by jointly clustering both images and tasks.

Directly training the meta learner to generate the weights for the feature embedding network can be challenging [3] since the prediction task requires predicting a large number of weights from a low dimensional task embedding with only a few training tasks. We therefore introduce a novel method to factorize the generated weights into small set of predicted weights and a larger set of shared weights.

The proposed architecture exceeds the state-of-the-art zero-shot learning on four standard benchmarks without the need for additional data generation. On the newly proposed visual-attribute composition task which is a more challenging zero-shot learning task, we are able to achieve an 4 to 15 point improvements over state-of-the-art discriminative models based on joint embedding. Our methods also achieve competitive results on the challenging few-shot learning benchmark based on ImageNet. Furthermore, the proposed model can be used for efficient inference on a per-input basis with little modification and exceeds the performance of prior models that focus on model sparsification.

2. Related Work

Weight generation. Several efforts [3, 16, 6] have studied the idea of adopting one meta network to generate weights

of another network. Our task-aware meta learner serves a similar role for the weight generation but in a more structured and constrained manner. We study different mechanisms to decompose the weights of the prediction network so that it can generate weights for multiple layers at once where Bertinetton *et al.* [3] focuses on generating weights for a single layer and Denil *et al.* [6] can generate up to 95% parameters of a single layer due to the quadratic size of the output space. As a byproduct of our design, we also study adding sparse constraints to the generated weights or efficient inference [28, 43, 45] and the resulting model outperforms the state-of-the-art dynamic channel pruning technique [28].

Joint embedding learning. Our architecture leverages common task and image embeddings to improve the task efficiency when learning the task embedding. This approach is commonly used in work on zero- and few- shot learning [25, 48, 41, 51, 4, 11]. A metric-learning based objective [25, 48, 41] is often used to jointly regularize the task embeddings and image embeddings for training the classification network while our embedding objective is used to address the data scarcity issue of the weight generation network.

Meta learning. Our work resides in the meta learning regime [9, 10, 36, 15] to learn the structure among previously seen tasks or concepts such that this learned prior can be combined with small amounts of new data for better generalization [9]. Our task-aware meta learner generalizes to new tasks with limited training data thanks to our novel embedding loss.

Feature modulation. In the domain of visual question answering, previous works [34, 5] explore the use of question embedding network to modulate the features of the

primary convolutional network. Our factorized weight generation scheme for convolutional layers can also be viewed as channel-wise feature modulation.

3. Task-Aware Feature Embedding

The choice of the featurization of data depends on the prediction tasks [7, 12]. For example, identifying whether images are underwater scenes or contain a particular digit relies on different representations (e.g., color or texture).

In many cases there is rich semantic meta-data describing the concept associated with a prediction task. For example, we might have text describing the objects of interest or the semantic meaning of the categories. Even the input image can be used to help characterize the prediction task. Encoding the prediction task as part of the learning problem can aid in generalization. Xian *et al.* [46] and Frome *et al.* [11] demonstrate that modeling the semantic relationship between tasks can help the model generalize to new tasks.

In this work, we explore a mechanism that can better incorporate the task specifications so that the model can learn and predict more efficiently. More specifically, we are interested in the design of models that can leverage meta-data describing the task to augment the data featurization.

To address this problem, we propose *Task-aware Feature Embedding* networks (TAFE-Nets) that generate feature embeddings conditioned on the task specification. We adopt a meta learning approach to construct TAFE-Nets by generating task-specific parameters for the prediction network and introduce two key innovations in weight factorization and embedding loss design to train TAFE-Nets effectively.

3.1. TAFE-Net Model

We start with the TAFE-Net design. There are two sub-networks in TAFE-Net as shown in Figure 2: a task-aware meta learner \mathcal{G} and a prediction network \mathcal{F} . The task-aware meta learner takes a task specification (e.g., word2vec [31] encoding or example image) \mathbf{t} and generates the weights of layers in the prediction network. The prediction network \mathcal{F} :

$$\mathbf{y} = \mathcal{F}(\mathbf{x}; \theta = \{\mathcal{G}(\mathbf{t}), \theta_f\}), \quad (1)$$

takes images or image features \mathbf{x} as inputs and predicts the class label $\mathbf{y} \in \{1 \dots N\}$. The prediction network \mathcal{F} is parameterized by θ which is composed of generated parameters from \mathcal{G} for task-aware feature embeddings and shared parameters θ_f that are shared across tasks (e.g., generic feature extraction). The task-aware feature embedding (TAFE) is the layer output of \mathcal{F} before the final classification layer.

The task-aware meta learner \mathcal{G} parameterized by η is composed of an embedding network $\mathcal{T}(\mathbf{t})$ to generate a latent task embedding \mathbf{e}_t and a set of weight generators $\mathbf{g}^i, i = \{1 \dots K\}$ that generate parameters for K feature layers in \mathcal{F} conditioned on \mathbf{e}_t .

3.2. Weight Generation via Factorization

We now present details of the weight generation scheme for the feature layers in \mathcal{F} . The feature layers that produce the task aware feature embeddings (TAFE) can either be convolutional layers or fully-connected (FC) layers. As noted by Bertinetto *et al.* [3], the number of weights that must be estimated by the meta-learner is often much larger than the task specifications and can therefore be difficult to learn from a small number of example tasks. To ensure meta learner generalizes effectively, we propose a weight factorization scheme along the output dimension of each FC layer and the output channel dimension of a convolutional layer. This is distinct from the low-rank decomposition used in prior meta-learning works [3]. The channel-wise factorization builds on the intuition that channels of a convolutional layer may have different or even orthogonal functionality.

Weight factorization for convolutions. Given an input tensor $\mathbf{x}^i \in \mathbb{R}^{w \times h \times c_{in}}$ for the i -th feature layer in \mathcal{F} whose weight is $\mathbf{W}^i \in \mathbb{R}^{k \times k \times c_{in} \times c_{out}}$ (k is the filter support size and c_{in} and c_{out} are the number of input and output channels) and bias is $\mathbf{b}^i \in \mathbb{R}^{c_{out}}$, the output $\mathbf{x}^{i+1} \in \mathbb{R}^{w' \times h' \times c_{out}}$ of the convolutional layer is given by

$$\mathbf{x}^{i+1} = \mathbf{W}^i * \mathbf{x}^i + \mathbf{b}^i, \quad (2)$$

where $*$ denotes convolution. Without loss of generality, we remove the bias term of the convolutional layer as it is often followed by the batch normalization [22]. $\mathbf{W}^i = \mathbf{g}^i(\mathbf{t})$ is the output of the i -th weight generator in \mathcal{G} . We decompose the weight \mathbf{W}^i into

$$\mathbf{W}^i = \mathbf{W}_{sr}^i *_{c_{out}} \mathbf{W}_{ts}^i, \quad (3)$$

where $\mathbf{W}_{sr}^i \in \mathbb{R}^{k \times k \times c_{in} \times c_{out}}$ is a shared parameter aggregating all tasks $\{\mathbf{t}_1, \dots, \mathbf{t}_N\}$ and $\mathbf{W}_{ts}^i \in \mathbb{R}^{1 \times 1 \times c_{out}}$ is a task-specific parameter depending on the current task input. $*_{c_{out}}$ denotes the grouped convolution along the output channel dimension, i.e. each channel of $x *_{c_{out}} y$ is simply the convolution of the corresponding channels in x and y .

Weight factorization for FCs. Similar to the factorization of the convolution weights, the FC layer weights $\mathbf{W}^i \in \mathbb{R}^{m \times n}$ can be decomposed into

$$\mathbf{W}^i = \mathbf{W}_{sr}^i \cdot \text{diag}(\mathbf{W}_{ts}^i), \quad (4)$$

where $\mathbf{W}_{sr}^i \in \mathbb{R}^{m \times n}$ is the shared parameters for all tasks and $\mathbf{W}_{ts}^i \in \mathbb{R}^n$ is the task-specific parameter.

With such factorization, the weight generators only need to generate the task-specific parameters for each task in lower dimension and learn one set of parameters in high dimension shared across all tasks.

3.3. Embedding Loss for Meta Learner

The number of task specifications used for training the task-aware meta learner is usually much smaller than the

number of images available for training the prediction network. The data scarcity issue may lead to a corrupted meta learner. We, therefore, propose to add a secondary *embedding loss* \mathcal{L}_{emb} for the meta learner alongside the standard classification loss \mathcal{L}_{cls} used for the prediction network. The overall objective is then defined as

$$\min_{\theta, \eta} \mathcal{L} = \min_{\theta, \eta} \mathcal{L}_{\text{cls}} + \beta \cdot \mathcal{L}_{\text{emb}}, \quad (5)$$

where β is the hyper-parameter to balance the two terms. We use β as 0.1 in our experiments if not specified.

The idea is to project the latent task embedding $\mathcal{T}(t)$ into a joint embedding space with the task-aware feature embedding (TAFE). We adopt a metric learning approach that for positive inputs of a given task, the corresponding TAFE is closer to the task embedding while for negative inputs, the corresponding TAFE is far from the task embedding as illustrated in Figure 1.

We use hinged cosine similarity as the distance measurement (i.e. $\mathcal{D}(p, q) = \max(\text{cosine_sim}(p, q), 0)$) and a regression loss defined as

$$\mathcal{L}_{\text{emb}} = \frac{1}{TS} \sum_i^T \sum_j^S \|\mathcal{D}(\text{TAFE}(\mathbf{x}_j; \mathbf{t}_i), \mathcal{T}(\mathbf{t}_i)) - \mathbf{q}_{i,j}\|_2^2, \quad (6)$$

where \mathbf{x}_j is the j -th sample in the dataset, \mathbf{t}_i is the i -th task and $\mathbf{q}_{i,j}$ is 1 if $\mathcal{F}(\mathbf{x}_j; \mathbf{t}_i)$ predicts positive and 0 otherwise. T and S is the total number of task descriptions and input samples respectively.

We find in experiments this additional supervision helps training the meta learner especially under the case where the number of training tasks is extremely limited.

3.4. Shallow Image Embedding as a Task Desc.

An interesting usage of task aware feature embeddings is to adapt the feature embedding to the input image itself. Moreover, the image that we are trying to classify provides some hints as to what is likely a good embedding for classifying that image. For example, having a hint as to the likely prediction or a high-level category is a form of task specifications that can inform the choice of image embedding.

In this work we also explore the use of task aware feature embeddings as a mechanism to construct more compact feature embeddings for traditional classification tasks. We find that with simple sparse constraints on the weight generator, our model can be used to construct a unique thin embedding network for each input image with only minimal loss in prediction accuracy.

In this setting, the task embedding network \mathcal{T} takes the image as the input and outputs a probabilistic assignment to the pre-defined tasks. That is to say, the embedding loss of the meta learner is defined using the cross-entropy loss with

sparse constraints over the output of the weight generators (K is the number of feature layers in the prediction network):

$$\mathcal{L}_{\text{emb}} = \frac{1}{S} \sum_j^S \text{CE}(\mathcal{T}(\mathbf{x}_j), \mathbf{y}_j) + \frac{1}{K} \sum_i^K \|\mathbf{g}^i(\mathcal{T}(\mathbf{x}_j))\|_1. \quad (7)$$

This soft assignment can be regarded as a task description for the image at hand. The computation for feature embedding can be reduced with the information from the meta network, since we can use the task description to decide which channels in each layer are related to the tasks of interest and which are not. To remove the irrelevant channels, we pass each of the generated parameters through a ReLU non-linearity. If a parameter is 0, we don't have to compute the activation map for that channel because all the parameters can be generated before any computation in feature network. This is similar to model cascading [42] if the meta and feature networks are both treated as making predictions. But in our case, the shallow network also generates weights for the more computation intensive network.

3.5. Model Configurations

We now describe the network configurations. In our work, we consider three types of task specifications: semantic representation in a vector format (e.g. word2vec [31] of the class labels), image features extracted from pre-trained models (the spacial dimension is collapsed) and raw images. For the first two cases detailed in Section 4, the task embedding network \mathcal{T} is a three-layer FC network with hidden unit size of 2048 except for the aPY dataset [8] where we choose \mathcal{T} as a 2-layer FC network with the same hidden size to avoid overfitting. The weight generator \mathbf{g}^i is a single FC layer with the output dimension same as the output dimension of the corresponding feature layer in \mathcal{F} . To enable efficient inference, we just add a ReLU to the output of \mathbf{g}^i . In the case where raw images are used as inputs, \mathcal{T} is configured as a 5-layer convolutional network with 3×3 kernels following the feature down-sampling schedule of ResNets [18].

For the prediction network, the TAFE is generated through a 3-layer FC network with the hidden size of 2048 if image features are extracted from pre-trained models and used as the input of the prediction network (on the aPY dataset, we use a 1024-1024-1024-2048 FC network to avoid overfitting). If raw images are used as the input, we will modify the backbone prediction network (e.g. VGG-16 [37] and ResNet-50 [18]) to generate the TAFE detailed in Section 4.4.

4. Experiments

We first conduct experiments using five zero-shot learning benchmark datasets: SUN, CUB, AWA1, AWA2 and aPY following the generalized zero-shot learning setting proposed by Xian *et al.* [46]. We also provide results on the

more challenging visual attributes composition task proposed by Misra *et al.* [32] on both MITStates [23] and StanfordVRD [29] datasets. Our model surpasses the state-of-the-art methods by a significant margin. We also evaluate the model on the few-shot learning and the dynamic model sparsification tasks on the CIFAR and ImageNet benchmarks and our model matches or exceeds the prior works.

4.1. Generalized Zero-shot Learning

The GZSL setting proposed by Xian *et al.* [46] is more realistic compared to the conventional zero-shot learning which involves classifying test examples from both seen and unseen classes, with no prior distinction between them. We compare our model with two lines of prior work in our experiments: (1) discriminative baselines [50, 48] which focus on mapping the images into a rich semantic embedding space, and (2) generative models [47, 40] that tackle the data scarcity problem by generating synthetic images for the unseen classes using a GAN [13, 52] based approach. Our work falls into the first category of research but we demonstrate in Table 2 that our approach is still competitive to the generative models with additional training data.

Datasets and evaluation metrics. Following prior works [51, 11, 1, 2], we conduct our experiments on 5 benchmark datasets (Table 1). We follow the evaluation metrics proposed by Xian *et al.* [46] to report the per class top-1 accuracy of both unseen acc_u and seen classes acc_s and the harmonic mean $H = 2 \times (acc_u \times acc_s) / (acc_u + acc_s)$.

Training details. We set the batch size to 32 and use Adam [24] as the optimizer with the initial learning rate of 10^{-4} for the prediction network and weight generators, and 10^{-5} for the task embedding network. We reduce the learning rate by $10\times$ at epoch 30 and 45, and train the network for 60 epochs. For AWA1, we train the network for 10 epochs and reduce the learning rate by $10\times$ at epoch 5.

Table 1: Datasets used in GZSL

Dataset	SUN	CUB	AWA1	AWA2	aPY
No. of Images	14,340	11,788	30,475	37,322	15,339
Attributes Dim.	102	312	85	85	64
\mathcal{Y}	717	200	50	50	32
\mathcal{Y}^{seen}	645	150	40	40	20
\mathcal{Y}^{unseen}	72	50	10	10	12
Granularity	fine	fine	coarse	coarse	coarse

Quantitative results. We first report the performance of our TAFE-Net w/o the proposed embedding loss in Table 2 compared to the non-generative models. Our best performing models surpass the prior models by a significant margin with an improvement of roughly 16 points on AWA1 and 17 points on aPY. For the more challenging fine-grained SUN and

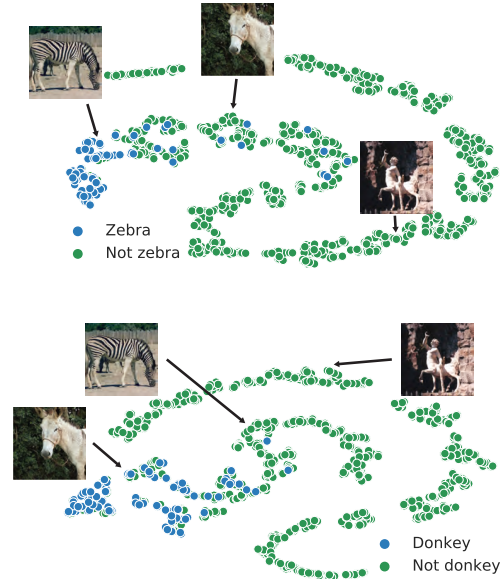


Figure 3: Task-aware Image Feature Embedding projected into two dimensions using t-SNE [39] for two tasks (Zebra and Donkey). Note that changing the task produces different embeddings for the same data.

CUB datasets, we are able to improve the results by 7 and 2 points. Compared to the more recent approaches [50, 48], our models have higher accuracy in the unseen classes which leads to the boost in the harmonic mean.

As an alternative approach to address the GZSL problem, Several [47, 40] propose to generate synthetic images of the unseen classes conditioned on the class attributes with variants of GAN models [14]. We show the comparison of our model with these generative models in Table 2. Our model matches or outperforms the baseline generative models on both CUB and AWA1 datasets without using additional training data. This indicates that better embedding learning may be more beneficial than the synthetic data generation. However, task aware embeddings and data generation are complementary and could be combined to further improve accuracy.

Embedding loss ablation. We provide numbers for our model w/o the embedding loss in Table 2. In general, models with the embedding loss have stronger performance than those without the embedding loss except for the SUN dataset whose number of categories is about $3 - 22\times$ larger than the other datasets. This observation matches our assumption that the additional supervision on the joint embedding better addresses the data scarcity issue (i.e. fewer class descriptions than the visual inputs) of training the controller model.

Embedding visualization. In Figure 3, we visualize the task-aware feature embeddings of images from the aPY

Table 2: Evaluate TAFE-Net on five standard benchmarks under generalized zero-shot learning setting. Models with \dagger (f-CLSWGAN and SE) generate additional data for training while the remaining models do not. Our model is better than all models without additional data and also competitive compared to models with additional synthetic data.

Method	SUN			CUB			AWA1			AWA2			aPY		
	u	s	H	u	s	H	u	s	H	u	s	H	u	s	H
LATEM [51]	14.7	28.8	19.5	15.2	57.3	24.0	7.3	71.7	13.3	11.5	77.3	20.0	0.1	73.0	0.2
ALE [1]	21.8	33.1	26.3	23.7	62.8	34.4	16.8	76.1	27.5	14.0	81.8	23.9	4.6	73.7	8.7
DeViSE[11]	16.9	27.4	20.9	23.8	53.0	32.8	13.4	68.7	22.4	17.1	74.7	27.8	4.9	76.9	9.2
SJE [2]	14.7	80.5	19.8	23.5	59.2	33.6	11.3	74.6	19.6	8.0	73.9	14.4	3.7	55.7	6.9
SYNC [4]	7.9	43.3	13.4	11.5	70.9	19.8	8.9	87.3	16.2	10.0	90.5	18.0	7.4	66.3	13.3
DEM [50]	20.5	34.3	25.6	19.6	57.9	29.2	32.8	84.7	47.3	30.5	86.4	45.1	11.1	75.1	19.4
RelationNet [48]	-	-	-	38.1	61.1	47.0	31.4	91.3	46.7	30.0	93.4	45.3	-	-	-
f-CLSWGAN \dagger [47]	-	-	-	57.7	43.7	49.7	61.4	57.9	59.6	-	-	-	-	-	-
SE \dagger [40]	-	-	-	53.3	41.5	46.7	67.8	56.3	61.5	-	-	-	-	-	-
TAFE-Net *	27.7	41.1	33.1	36.5	60.0	45.4	46.1	81.4	58.8	31.9	91.2	47.2	19.4	71.3	30.5
TAFE-Net	27.9	40.2	33.0	41.0	61.4	49.2	50.5	84.4	63.2	36.7	90.6	52.2	24.3	75.4	36.8

dataset. As we can see, image embeddings are projected into different clusters conditioned on the task specification.

4.2. Unseen Visual-attribute Composition

Besides the standard zero-shot learning benchmarks, we evaluate our model in the visual-attribute composition task proposed by Misra *et al.* [32]. The goal is to compose a set of visual concept primitives like attributes and objects (e.g. large elephant, old building, etc.) to obtain new visual concepts for a given image. We see this task as a more challenging “zero-shot” learning task which requires the model not only to predict unseen visual concept compositions but model the contextuality of the concepts.

Datasets and evaluation metrics. We conduct the experiments on two datasets: MITStates [23] and the modified StanfordVRD [29]. The setup is the same as Misra *et al.* [32]. Each image in the MITStates dataset is assigned a pair of (attribute, object) as its label. The model is trained on 34K images with 1,292 label pairs and tested on 19K images with 700 unseen pairs. The second dataset is constructed based on the bounding boxes annotations of the StanfordVRD dataset. Each sample has an SPO (subject, predicate, object) tuple as the ground truth label. The dataset has 7,701 SPO tuples and 1,029 of them are seen only in the test split. We evaluate our models only on examples with unseen labels. We extract the image features with pre-trained models on ImageNet. We use ResNet-101 [18] as our main feature extractor and also test features extracted with ResNet-18 [18], VGG-16/19 [37] for ablation. For the task specifications, we concatenate the word embeddings of the attributes and objects with word2vec [31] trained with GoogleNews. We also consider one-hot encoding for the task id in the ablation.

For evaluation metrics, we report the mean Average Precision (mAP) of images with unseen labels in the test set together with the top- k accuracy where $k = 1, 2, 3$. We follow the same training schedule as that used in GZSL.

Quantitative results. We compare our model with several baselines provided by Misra *et al.* [32] and summarize the results in Table 3 for both MITStates and StanfordVRD datasets. Our model surpasses the state-of-the-art models with an improvement of more than 6 points in mAP and 4 to 15 points in top- k accuracy. Nagarajan and Grauman [33] recently propose an embedding learning framework for visual-attribute composition. They report the top-1 accuracy of 12.0% on the MITStates dataset with ResNet-18 features. For fair comparison, we use the same ResNet-18 features and obtain the top-1 accuracy of 15.1%.

Ablation on the feature extractor and task specification. We consider different feature extractors (ResNet-101, VGG-16 and 19) and task encodings (word2vec and one-hot encoding) for ablation and summarize the results in Table 4. The average precision difference between different feature extractors are very minimal (within 0.1%) and the largest gap in Top-3 accuracy is within 2%. This indicates that TAFE-Net is robust in transforming the generic features into task-aware feature embeddings. For the task encoding, the one-hot encoding is comparable to the word2vec encoding and even stronger when using VGG-19 features. This shows that the task transformer network \mathcal{T} is very expressive to extract rich semantic information simply from the task ids.

Visualization. In Figure 4, we show the top retrievals of unseen attribute-object pairs from the MITStates dataset. Our model can learn to compose new concepts from the

Table 3: Evaluation on 700 unseen (attribute, object) pairs on 19K images of the MITStates Dataset and 1029 unseen SPO tuples on 1000 images of the StanfordVRD Dataset. TAFE-Net improves over the baselines by a large margin.

Method	MITStates				StanfordVRD			
	AP	Top- <i>k</i> Accuracy			AP	Top- <i>k</i> Accuracy		
		1	2	3		1	2	3
Visual Product [32]	8.8	9.8	16.1	20.6	4.9	3.2	5.6	7.6
Label Embed (LE) [32]	7.9	11.2	17.6	22.4	4.3	4.1	7.2	10.6
LEOR [32]	4.1	4.5	6.2	11.8	0.9	1.1	1.3	1.3
LE + R [32]	6.7	9.3	16.3	20.8	3.9	3.9	7.1	10.4
Red Wine [32]	10.4	13.1	21.2	27.6	5.7	6.3	9.2	12.7
TAFE-Net	16.2	16.9	27.9	35.1	12.2	12.3	19.7	27.5

Table 4: Ablation study with different task encoding and base network features. The variance of performance of TAFE-Net under different settings is minimal.

Task Encoding	Features	AP	Top- <i>k</i> Accuracy		
			1	2	3
Word2vec	ResNet-101	16.2	17.2	27.8	35.7
Onehot	ResNet-101	16.1	16.1	26.8	33.8
Word2vec	VGG16	16.3	16.4	26.4	33.0
Onehot	VGG16	16.3	16.4	25.9	32.5
Word2vec	VGG19	15.6	16.2	26.0	32.4
Onehot	VGG19	16.3	16.4	26.0	33.1

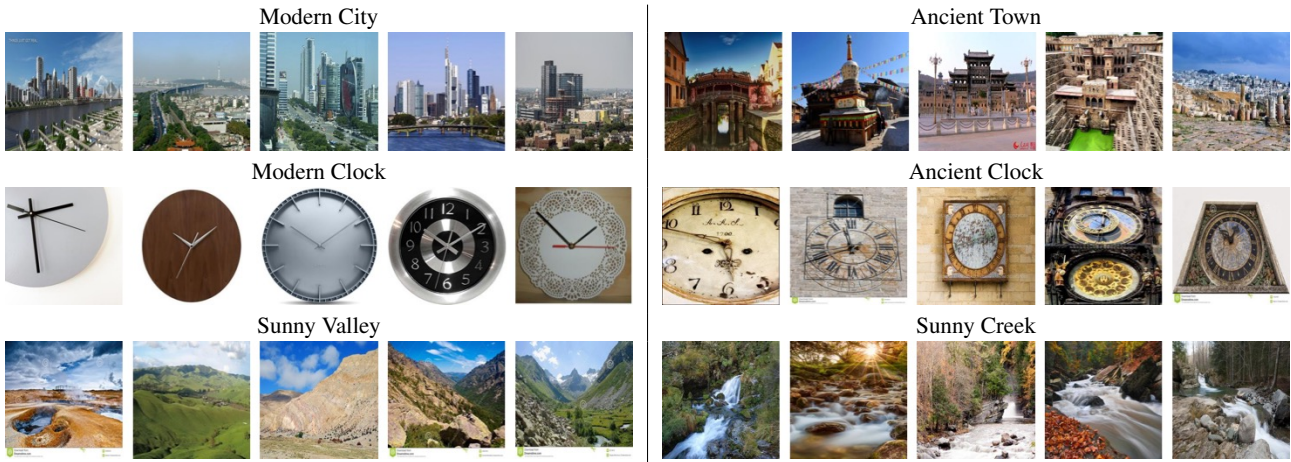


Figure 4: Top retrievals on the unseen pairs of the MITStates dataset. Our model can learn to compose new concepts from the existing attributes and objects while respecting their context. The second row shows some of the failure cases.

existing attributes and objects while respecting their context.

4.3. Low-shot Image Classification

Our model naturally fits the few-shot learning setting where one or few images of a certain category are used as the task descriptions. Unlike prior work on meta-learning which experiments with few classes and low resolution images [41, 38, 10], we evaluate our model on the challenging benchmark proposed by Hariharan and Girshick [17]. The benchmark is based on the ImageNet images and contains hundreds of classes that are divided into base classes and novel classes. At inference time, the model is provided with one or a few examples from the novel classes and hundreds of examples from the base classes. The goal is to obtain high accuracy on the novel classes without sacrificing the performance on the base classes.

Baselines. In our experiments, the baselines we consider are the state-of-the-art meta learning models Matching Network (MN) [41] and Prototypical Network (PN) [38]. We also

compare the logistic regression (LogReg) baseline provided by Hariharan and Girshick [17]. Another line of research [44, 17] for few-shot learning is to combine the meta-learner with a “hallucinator” to generate additional training data. We regard these works as complementary approaches to our meta-learning model.

Experiment details. We follow the prior works [17, 44] to run five trials for each setting of *n* (the number of examples per novel class, *n* = 1 and 2 in our experiments) on the five different data splits and report the average top-5 accuracy of both the novel and all classes. We use the features trained with ResNet-10 using SGM loss provided by Hariharan and Girshick [17] as inputs. For training, we sample 100 classes in each iteration and use SGD with momentum of 0.9 as the optimizer. The initial learning rate is set to 0.1 except for the task embedding network (set to 0.01) and the learning rate is reduced by 10× every 8k iterations. The model is trained for 30k iterations in total. Other hyper-parameters are set to the same as Hariharan and Girshick [17] if not mentioned.

Table 5: Few-shot ImageNet Classification on ImageNet. Our model is competitive compared to the state-of-the-art meta learning model without hallucinator.

Method	Novel Top-5 Acc		All Top-5 Acc	
	n=1	n=2	n=1	n=2
LogReg [17]	38.4	51.1	40.8	49.9
PN [38]	39.3	54.4	49.5	61.0
MN [41]	43.6	54.0	54.4	61.0
TAFE-Net	43.0	53.9	55.7	61.9
LogReg w/ Analogies [17]	40.7	50.8	52.2	59.4
PN w/ G [44]	45.0	55.9	56.9	63.2

Quantitative results. As shown in Table 5, our model is on par with the state-of-the-art meta learning models in the novel classes while outperforming them in all categories. Attaching a “hallucinator” to the meta learning model improves performance in general. Our model can be easily attached with a hallucinator and we leave the detailed study as future work due to the time constraint.

4.4. Efficient Inference in Data-Rich Classification

As noted in Section 3.4, the task embedding network and the feature embedding network can share the same input image. In this case, the shallow embedding of the input image can be treated as a “task” and conditioned on it, and the weight generator network generates weights that are customized for the given input. Adding additional sparse constraints to the generated weights, our model can be used to selectively sparsify the channels of the convolutional layers of the prediction network on a per-input basis. This is in line with prior works [28, 30, 19] on channel pruning and we demonstrate that with a slight change in the weight generator (adding sparsity constraints), our model is competitive with or beats existing work on model sparsification.

Baselines. The closest baseline is the runtime neural pruning (RNP) proposed by Lin *et al.* [28], which dynamically prunes the channels of the subsequent convolutional layers based on the previous layer outputs. We compare with RNP on the CIFAR-100 [26] dataset using VGG-16 as the backbone following the setting as Lin *et al.* [28]. We also consider state-of-the-art static channel pruning works [19, 30, 21, 27], with ResNet-50 on the ImageNet-2012 [35] dataset.

Sparse weight generation for residual blocks. For the bottleneck residual block used in ResNet-50 [18] which has 3 convolutional layers with the kernel filter size of 1, 3 and 1, we only generate sparse weights for the middle convolutional layer which is the computation bottleneck and share the weights of the first and last layer across inputs.

Training details. For the CIFAR dataset, we start training with the learning rate of 0.1 for ResNet and 0.01 for VGG16,

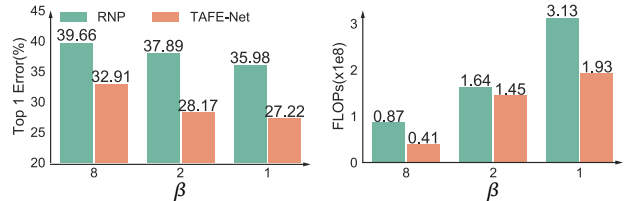


Figure 5: Comparison of TAFE-Net and RNP with VGG-16 on CIFAR-100. Our model outperforms RNP under different accuracy and computation trade-off. β controls the amount of the L1 regularization in Equation 7.

Table 6: Pruned ResNet-50 on ImageNet. Top-1/5 error rate and computation FLOPs are reported. Our model achieves lower error rate with lower computational cost.

Model	Top-1	Top-5	FLOPs(x10 ⁹)	Reduct.(%)
SSS [21]	26.8	-	3.0	20.3
Li et al. [27]	27.0	8.9	3.0	19.0
He et al. [19]	-	9.2	1.9	50.0
ThiNet [30]	29.0	10.0	1.7	55.8
TAFE-Net	26.2	8.4	1.6	56.8

which is reduced by 10 \times at the 150th and 250th epochs with total 350 epochs for the baselines and 270 epochs for TAFE-Net joint optimization stage and another 80 epochs for fine-tuning with fixed task embedding networks. For ImageNet, we train the network with the initial learning rate of 0.1 for 100 epochs and reduce it by 10 \times every 30 epochs.

Quantitative results. We summarize our comparison with the baselines in Figure 5 and Table 6. Our approach outperforms the previous baselines to achieve higher accuracy with lower runtime computation measured in floating point operations per second (FLOPs).

5. Conclusion

In this work, we explored a meta learning based approach to generate task aware feature embeddings for settings with little or no training data. We proposed TAFE-Net, a network that generates task aware feature embeddings (TAFE) conditioned on the given task descriptions. TAFE-Net is composed of a task-aware meta learner that generates weights for the feature embedding layers in a standard prediction network. To address the challenges in training the meta learner, we introduced two key innovations: (1) adding an additional embedding loss to improve the generalization of the meta learner; (2) a novel weight factorization scheme to generate parameters of the prediction network more effectively. We demonstrated the general applicability of the proposed network design on a range of applications including zero/few shot learning and dynamic efficient prediction, and exceeded or matched the state-of-the-art on most applications.

References

- [1] Z. Akata, F. Perronnin, Z. Harchaoui, and C. Schmid. Label-embedding for image classification. *IEEE transactions on pattern analysis and machine intelligence*, 38(7):1425–1438, 2016. [5](#), [6](#)
- [2] Z. Akata, S. Reed, D. Walter, H. Lee, and B. Schiele. Evaluation of output embeddings for fine-grained image classification. In *Proceedings of the IEEE Conference on Computer Vision and Pattern Recognition*, pages 2927–2936, 2015. [5](#), [6](#)
- [3] L. Bertinetto, J. F. Henriques, J. Valmadre, P. Torr, and A. Vedaldi. Learning feed-forward one-shot learners. In *Advances in Neural Information Processing Systems*, pages 523–531, 2016. [2](#), [3](#)
- [4] S. Changpinyo, W.-L. Chao, B. Gong, and F. Sha. Synthesized classifiers for zero-shot learning. In *The IEEE Conference on Computer Vision and Pattern Recognition (CVPR)*, June 2016. [1](#), [2](#), [6](#)
- [5] H. De Vries, F. Strub, J. Mary, H. Larochelle, O. Pietquin, and A. C. Courville. Modulating early visual processing by language. In *Advances in Neural Information Processing Systems*, pages 6594–6604, 2017. [2](#)
- [6] M. Denil, B. Shakibi, L. Dinh, N. De Freitas, et al. Predicting parameters in deep learning. In *Advances in neural information processing systems*, pages 2148–2156, 2013. [2](#)
- [7] J. Donahue, Y. Jia, O. Vinyals, J. Hoffman, N. Zhang, E. Tzeng, and T. Darrell. Decaf: A deep convolutional activation feature for generic visual recognition. In *International conference on machine learning*, pages 647–655, 2014. [1](#), [3](#)
- [8] A. Farhadi, I. Endres, D. Hoiem, and D. Forsyth. Describing objects by their attributes. In *Computer Vision and Pattern Recognition, 2009. CVPR 2009. IEEE Conference on*, pages 1778–1785. IEEE, 2009. [4](#)
- [9] C. Finn. *Learning to Learn with Gradients*. PhD thesis, UC Berkeley, 2018. [2](#)
- [10] C. Finn, P. Abbeel, and S. Levine. Model-agnostic meta-learning for fast adaptation of deep networks. *ICML*, 2017. [2](#), [7](#)
- [11] A. Frome, G. S. Corrado, J. Shlens, S. Bengio, J. Dean, T. Mikolov, et al. DeViSe: A deep visual-semantic embedding model. In *Advances in neural information processing systems*, pages 2121–2129, 2013. [1](#), [2](#), [3](#), [5](#), [6](#)
- [12] R. Girshick, J. Donahue, T. Darrell, and J. Malik. Rich feature hierarchies for accurate object detection and semantic segmentation. In *Proceedings of the IEEE conference on computer vision and pattern recognition*, pages 580–587, 2014. [1](#), [3](#)
- [13] I. Goodfellow, J. Pouget-Abadie, M. Mirza, B. Xu, D. Warde-Farley, S. Ozair, A. Courville, and Y. Bengio. Generative adversarial nets. In *Advances in neural information processing systems*, pages 2672–2680, 2014. [5](#)
- [14] I. Goodfellow, J. Pouget-Abadie, M. Mirza, B. Xu, D. Warde-Farley, S. Ozair, A. Courville, and Y. Bengio. Generative adversarial nets. In Z. Ghahramani, M. Welling, C. Cortes, N. D. Lawrence, and K. Q. Weinberger, editors, *Advances in Neural Information Processing Systems 27*, pages 2672–2680. Curran Associates, Inc., 2014. [5](#)
- [15] A. Graves, G. Wayne, and I. Danihelka. Neural turing machines. *arXiv preprint arXiv:1410.5401*, 2014. [2](#)
- [16] D. Ha, A. Dai, and Q. V. Le. Hypernetworks. *arXiv preprint arXiv:1609.09106*, 2016. [2](#)
- [17] B. Hariharan and R. Girshick. Low-shot visual recognition by shrinking and hallucinating features. In *2017 IEEE International Conference on Computer Vision (ICCV)*, pages 3037–3046. IEEE, 2017. [1](#), [7](#), [8](#)
- [18] K. He, X. Zhang, S. Ren, and J. Sun. Deep residual learning for image recognition. In *Proceedings of the IEEE conference on computer vision and pattern recognition*, pages 770–778, 2016. [1](#), [4](#), [6](#), [8](#)
- [19] Y. He, X. Zhang, and J. Sun. Channel pruning for accelerating very deep neural networks. In *International Conference on Computer Vision (ICCV)*, volume 2, page 6, 2017. [8](#)
- [20] J. Hoffman, E. Tzeng, T. Park, J.-Y. Zhu, P. Isola, K. Saenko, A. A. Efros, and T. Darrell. Cycada: Cycle consistent adversarial domain adaptation. In *International Conference on Machine Learning (ICML)*, 2018. [1](#)
- [21] Z. Huang and N. Wang. Data-driven sparse structure selection for deep neural networks. *arXiv preprint arXiv:1707.01213*, 2017. [8](#)
- [22] S. Ioffe and C. Szegedy. Batch normalization: Accelerating deep network training by reducing internal covariate shift. *arXiv preprint arXiv:1502.03167*, 2015. [3](#)
- [23] P. Isola, J. J. Lim, and E. H. Adelson. Discovering states and transformations in image collections. In *CVPR*, 2015. [5](#), [6](#)
- [24] D. P. Kingma and J. Ba. Adam: A method for stochastic optimization. *arXiv preprint arXiv:1412.6980*, 2014. [5](#)
- [25] G. Koch. Siamese neural networks for one-shot image recognition. 2015. [2](#)
- [26] A. Krizhevsky and G. Hinton. Learning multiple layers of features from tiny images. 2009. [8](#)
- [27] H. Li, A. Kadav, I. Durdanovic, H. Samet, and H. P. Graf. Pruning filters for efficient convnets. *International Conference on Learning Representations*, 2017. [8](#)
- [28] J. Lin, Y. Rao, J. Lu, and J. Zhou. Runtime neural pruning. In *Advances in Neural Information Processing Systems*, pages 2178–2188, 2017. [2](#), [8](#)
- [29] C. Lu, R. Krishna, M. Bernstein, and L. Fei-Fei. Visual relationship detection with language priors. In *European Conference on Computer Vision*, 2016. [1](#), [5](#), [6](#)
- [30] J.-H. Luo, J. Wu, and W. Lin. ThiNet: A filter level pruning method for deep neural network compression. In *Proceedings of the IEEE Conference on Computer Vision and Pattern Recognition*, pages 5058–5066, 2017. [8](#)
- [31] T. Mikolov, K. Chen, G. Corrado, and J. Dean. Efficient estimation of word representations in vector space. *ICLR*, 2013. [3](#), [4](#), [6](#)
- [32] I. Misra, A. Gupta, and M. Hebert. From red wine to red tomato: Composition with context. In *CVPR*, volume 2, page 6, 2017. [5](#), [6](#), [7](#)
- [33] T. Nagarajan and K. Grauman. Attributes as operators. *ECCV*, 2018. [6](#)
- [34] E. Perez, F. Strub, H. de Vries, V. Dumoulin, and A. C. Courville. Film: Visual reasoning with a general conditioning layer. In *AAAI*, 2018. [2](#)

- [35] O. Russakovsky, J. Deng, H. Su, J. Krause, S. Satheesh, S. Ma, Z. Huang, A. Karpathy, A. Khosla, M. Bernstein, et al. Imagenet large scale visual recognition challenge. *International Journal of Computer Vision*, 115(3):211–252, 2015. 1, 8
- [36] J. Schmidhuber. *Evolutionary principles in self-referential learning, or on learning how to learn: the meta-meta-... hook*. PhD thesis, Technische Universität München, 1987. 2
- [37] K. Simonyan and A. Zisserman. Very deep convolutional networks for large-scale image recognition. *arXiv preprint arXiv:1409.1556*, 2014. 4, 6
- [38] J. Snell, K. Swersky, and R. Zemel. Prototypical networks for few-shot learning. In *Advances in Neural Information Processing Systems*, pages 4077–4087, 2017. 7, 8
- [39] L. van der Maaten and G. Hinton. Visualizing data using t-SNE. *Journal of Machine Learning Research*, 9:2579–2605, 2008. 5
- [40] V. K. Verma, G. Arora, A. Mishra, and P. Rai. Generalized zero-shot learning via synthesized examples. 5, 6
- [41] O. Vinyals, C. Blundell, T. Lillicrap, D. Wierstra, et al. Matching networks for one shot learning. In *Advances in Neural Information Processing Systems*, pages 3630–3638, 2016. 1, 2, 7, 8
- [42] X. Wang, Y. Luo, D. Crankshaw, A. Tumanov, F. Yu, and J. E. Gonzalez. Idk cascades: Fast deep learning by learning not to overthink. *UAI*, 2018. 4
- [43] X. Wang, F. Yu, Z.-Y. Dou, and J. E. Gonzalez. SkipNet: Learning dynamic routing in convolutional networks. *arXiv preprint arXiv:1711.09485*, 2017. 2
- [44] Y.-X. Wang, R. Girshick, M. Hebert, and B. Hariharan. Low-shot learning from imaginary data. *CVPR*, 2018. 1, 7, 8
- [45] Z. Wu, T. Nagarajan, A. Kumar, S. Rennie, L. S. Davis, K. Grauman, and R. Feris. Blockdrop: Dynamic inference paths in residual networks. 2018. 2
- [46] Y. Xian, C. H. Lampert, B. Schiele, and Z. Akata. Zero-shot learning—a comprehensive evaluation of the good, the bad and the ugly. *IEEE transactions on pattern analysis and machine intelligence*, 2018. 3, 4, 5
- [47] Y. Xian, T. Lorenz, B. Schiele, and Z. Akata. Feature generating networks for zero-shot learning. In *Proc. of the IEEE Conference on Computer Vision and Pattern Recognition (CVPR)*, Salt Lake City, UT, USA, 2018. 1, 5, 6
- [48] F. S. Y. Yang, L. Zhang, T. Xiang, P. H. Torr, and T. M. Hospedales. Learning to compare: Relation network for few-shot learning. In *Proc. of the IEEE Conference on Computer Vision and Pattern Recognition (CVPR)*, Salt Lake City, UT, USA, 2018. 2, 5, 6
- [49] M. D. Zeiler and R. Fergus. Visualizing and understanding convolutional networks. In *European conference on computer vision*, pages 818–833. Springer, 2014. 1
- [50] L. Zhang, T. Xiang, and S. Gong. Learning a deep embedding model for zero-shot learning. In *Proceedings of the IEEE Conference on Computer Vision and Pattern Recognition*, 2017. 5, 6
- [51] Z. Zhang and V. Saligrama. Zero-shot learning via joint latent similarity embedding. In *Proceedings of the IEEE Conference on Computer Vision and Pattern Recognition*, pages 6034–6042, 2016. 1, 2, 5, 6
- [52] J.-Y. Zhu, T. Park, P. Isola, and A. A. Efros. Unpaired image-to-image translation using cycle-consistent adversarial networks. *arXiv preprint*, 2017. 5